Elsevier Editorial System(tm) for Journal of Alloys and Compounds
Manuscript Draft

Manuscript Number: JALCOM-D-13-01826R1

Title: Modification of the α-Ti laths to near equiaxed α-Ti grains in as-sintered titanium and titanium alloys by a small addition of boron

Article Type: Letter

Keywords: Keywords: Titanium alloys; Powder Metallurgy; Grain refinement; Sintering; Metals and alloys

Corresponding Author: Dr. Yafeng Yang,

Corresponding Author's Institution:

First Author: Yafeng Yang

Order of Authors: Yafeng Yang; M. Yan; S.D. Luo; G.B. Schaffer; M. Qian

Abstract: A small addition of boron (B) changes the morphology of the α-Ti laths in as-sintered Ti-6Al-4V and Ti-10V-2Fe-3Al to near equiaxed α-Ti grains and increases the number density of the resulting □-Ti grains by up to six folds. TiB forms at about 700°C during heating to the isothermal sintering temperature and more than 90% of the TiB particles were found inside the α-Ti grains. Transmission electron microscopy (TEM) was used to identify the orientation relationships (ORs) between the TiB and α-Ti phases. Their exact ORs are affected by both the chemistry of the alloy and the processing conditions. The modification of the α-Ti laths and the substantial increase in the number density of the □-Ti grains are attributed to the enhanced heterogeneous nucleation of α-Ti on TiB due to the identified specific ORs and excellent lattice matches between these two phases. In addition, there exists a unique peritectoid reaction between β-Ti and TiB during the subsequent cooling after isothermal sintering by which β-Ti + TiB → α-Ti, which may have contributed to the enhanced heterogeneous nucleation of α-Ti on TiB.

Dear Editor:

The revised manuscript, entitled “Modification of the α-Ti laths to near equiaxed α-Ti grains in as-sintered titanium and titanium alloys by a small addition of boron”, is being resubmitted for possible publication.

We appreciate the very constructive comments and suggestions received. A detailed response to each question is given below. The manuscript has been revised accordingly with all amendments being underlined in the revised version.

We will be grateful to you for your review and comments on our manuscript again.

Yours sincerely,

Y.F. Yang

Research Fellow

E-mail: y.yang6@uq.edu.au

The University of Queensland, School of Mechanical and Mining Engineering, Australia.

Response to comments and suggestions

We appreciate the constructive comments and suggestions received. A detailed response to each question is given below. The manuscript has been revised accordingly, with all amendments being underlined in the revised version.

Reviewer's comments:

* *Fig. 1: The authors should add some consideration and comment about the presence and the identification of TiB particles in the microstructure. How did the authors identify the TiB phase? It would be interesting to add some other SEM images where it is shown the distribution of TiB particles in the phases*.

Response:

Identification of the TiB phase: The identification was based on TEM. Ti and B may form different forms of borides including TiB, Ti_3B_4 and TiB_2 according to the Ti-B phase diagram depending on the concentration of B and temperature. In the present study, small additions of B resulted in the formation of TiB, rather than TiB_2. The TEM results in Figure 3 confirmed this, where selected area electron diffraction (SAED) patterns showed a typical orthorhombic crystal structure of TiB. These comments have been added to the revised manuscript.

SEM images showing the distribution of the TiB particles: We have separated Figs. 1(c), 1(f) and 1(i) from Figs. 1(b), 1(e) and 1(h) and have enlarged each micrograph. These micrographs give a clear view about the distribution of the TiB particles in the microstructure.

* *Fig. 2 (c-d): It is not explained (in the "material and methods" and in the "results and discussion") how the authors have calculated the distribution of TiB in the different phases.*
The abstract should be expanded.

Response: We have added the following to the Section of "Results and discussion":

The in situ formed TiB particles were observed at two primary locations in each as-sintered microstructure: inside the α-Ti grains and outside the α-Ti grains. In as-sintered CP-Ti, being outside the α-Ti grains means being present along the prior-β grain boundaries while in as-sintered Ti-6Al-4V and Ti-10V-2Fe-3Al alloys being outside the α-Ti grains means being inside the β-Ti grains. The distribution of the TiB particles in different phases was quantified according to this principle.

The abstract has been expanded as follows:

A small addition of boron (B) changes the morphology of the α-Ti laths in as-sintered Ti-6Al-4V and Ti-10V-2Fe-3Al to near equiaxed α-Ti grains and increases the number density of the resulting α-Ti grains by up to six folds. TiB forms at about 700°C during heating to the isothermal sintering temperature and more than 90% of the TiB particles were found inside the α-Ti grains. Transmission electron microscopy (TEM) was used to identify the orientation relationships (ORs) between the TiB and α-Ti phases. Their exact ORs are affected by both the chemistry of the alloy and the processing conditions. The modification of the α-Ti laths and the substantial increase in the number density of the α-Ti grains are attributed to the enhanced heterogeneous nucleation of α-Ti on TiB due to the identified specific ORs and excellent lattice matches between these two phases. In addition, there exists a unique peritectoid reaction between β-Ti and TiB during the subsequent cooling after isothermal sintering by which β-Ti + TiB → α-Ti, which may have contributed to the enhanced heterogeneous nucleation of α-Ti on TiB.

In addition, we have added:

Acknowledgements - This work was funded by the Australian Research Council (ARC) through an Australian Postdoctoral Fellowship for Dr. Y. F. Yang and the Centre of Excellence for Design in Light Metals.

All new additions or amendments made to the revised manuscript have been underlined.

In α-β or near β Ti alloys, the morphology of the α-Ti phase exerts an important influence on the ductility of the alloy, where acicular α-Ti imparts lower ductility than equiaxed or globular α-Ti. As a result, thermo-mechanical processing is often used to change the morphology of the α-Ti phase. The modification effect of B offers a different approach to the control of the morphology of the α-Ti phase in as-sintered PM Ti materials. In this paper, we firstly reported quantitative experimental analyses and gave detailed theoretical support. Most of the TiB particles observed in the as-sintered Ti alloys were located inside the α-Ti grains. TEM characterization identified specific orientation relationships between TiB and α-Ti. A unique peritectoid reaction by which β-Ti + TiB → α-Ti offered an ideal route to enhance heterogeneous nucleation effect of α-Ti on TiB and modify the α-Ti laths to near equiaxed α-Ti grains.

Response to comments and suggestions

We appreciate the constructive comments and suggestions received. A detailed response to each question is given below. The manuscript has been revised accordingly, with all amendments being underlined in the revised version.

Reviewer's comments:

* *Fig. 1: The authors should add some consideration and comment about the presence and the identification of TiB particles in the microstructure. How did the authors identify the TiB phase? It would be interesting to add some other SEM images where it is shown the distribution of TiB particles in the phases*.

Response:

Identification of the TiB phase: The identification was based on TEM. Ti and B may form different forms of borides including TiB, Ti_3B_4 and TiB_2 according to the Ti-B phase diagram depending on the concentration of B and temperature. In the present study, small additions of B resulted in the formation of TiB, rather than TiB_2. The TEM results in Figure 3 confirmed this, where selected area electron diffraction (SAED) patterns showed a typical orthorhombic crystal structure of TiB. These comments have been added to the revised manuscript.

SEM images showing the distribution of the TiB particles: We have separated Figs. 1(c), 1(f) and 1(i) from Figs. 1(b), 1(e) and 1(h) and have enlarged each micrograph. These micrographs give a clear view about the distribution of the TiB particles in the microstructure.

* *Fig. 2 (c-d): It is not explained (in the "material and methods" and in the "results and discussion") how the authors have calculated the distribution of TiB in the different phases.*
The abstract should be expanded.

Response: We have added the following to the Section of “Results and discussion”:

The in situ formed TiB particles were observed at two primary locations in each as-sintered microstructure: inside the α-Ti grains and outside the α-Ti grains. In as-sintered CP-Ti, being outside the α-Ti grains means being present along the prior-β grain boundaries while in as-sintered Ti-6Al-4V and Ti-10V-2Fe-3Al alloys being outside the α-Ti grains means being inside the β-Ti grains. The distribution of the TiB particles in different phases was quantified according to this principle.

The abstract has been expanded as follows:

A small addition of boron (B) changes the morphology of the α-Ti laths in as-sintered Ti-6Al-4V and Ti-10V-2Fe-3Al to near equiaxed α-Ti grains and increases the number density of the resulting α-Ti grains by up to six folds. TiB forms at about 700°C during heating to the isothermal sintering temperature and more than 90% of the TiB particles were found inside the α-Ti grains. Transmission electron microscopy (TEM) was used to identify the orientation relationships (ORs) between the TiB and α-Ti phases. Their exact ORs are affected by both the chemistry of the alloy and the processing conditions. The modification of the α-Ti laths and the substantial increase in the number density of the α-Ti grains are attributed to the enhanced heterogeneous nucleation of α-Ti on TiB due to the identified specific ORs and excellent lattice matches between these two phases. In addition, there exists a unique peritectoid reaction between β-Ti and TiB during the subsequent cooling after isothermal sintering by which β-Ti + TiB → α-Ti, which may have contributed to the enhanced heterogeneous nucleation of α-Ti on TiB.

In addition, we have added:

Acknowledgements - This work was funded by the Australian Research Council (ARC) through an Australian Postdoctoral Fellowship for Dr. Y. F. Yang and the Centre of Excellence for Design in Light Metals.

Modification of the α-Ti laths to near equiaxed α-Ti grains in as-sintered titanium and titanium alloys by a small addition of boron

Y. F. Yang, M. Yan, S. D. Luo, G. B. Schaffer and M. Qian∗

The University of Queensland, School of Mechanical and Mining Engineering, ARC Centre of Excellence for Design in Light Metals, Brisbane, Qld 4072, Australia

Abstract

A small addition of boron (B) changes the morphology of the α-Ti laths in as-sintered Ti-6Al-4V and Ti-10V-2Fe-3Al to near equiaxed α-Ti grains and increases the number density of the resulting α-Ti grains by up to six folds. TiB forms at about 700°C during heating to the isothermal sintering temperature and more than 90% of the TiB particles were found inside the α-Ti grains. Transmission electron microscopy (TEM) was used to identify the orientation relationships (ORs) between the TiB and α-Ti phases. Their exact ORs are affected by both the chemistry of the alloy and the processing conditions. The modification of the α-Ti laths and the substantial increase in the number density of the α-Ti grains are attributed to the enhanced heterogeneous nucleation of α-Ti on TiB due to the identified specific ORs and excellent lattice matches between these two phases. In addition, there exists a unique peritectoid reaction between β-Ti and TiB during the subsequent cooling after isothermal sintering by which β-Ti + TiB → α-Ti, which may have contributed to the enhanced heterogeneous nucleation of α-Ti on TiB.

Keywords: Titanium alloys; Powder Metallurgy; Grain refinement; Sintering

∗Corresponding author, e-mail address: ma.qian@uq.edu.au

1. Introduction

A small addition of elemental boron (B) or borides refines the microstructure of as-sintered commercially pure Ti (CP-Ti) and Ti alloys and modifies the morphology of the α-Ti phase [1-4]. Marty et al. [1] first introduced a trace amount of B powder (160 ppm) or borides (B_4C and B_4Si) to powder metallurgy (PM) Ti alloys and observed noticeable grain refinement of the resulting prior-β grains. In a subsequent seminal paper, Saito [2] mentioned that an addition of 0.2%TiB_2 (in wt.% throughout) to blended elemental Ti-6Al-4V-1Mo produced noticeable structural refinement but no details were given. Recently, Ferri et al. [3] reported that as-sintered pre-alloyed (PA) Ti-6Al-4V-0.5B achieved a much finer microstructure than as-sintered PA Ti-6Al-4V leading to much improved mechanical properties including the fatigue strength. More recently, Luo et al. [4] showed that an addition of ≥0.31%B to a PM Ti-7Ni alloy (elemental blends) dramatically changed the morphology of the α-Ti phase from long laths to dispersed particulates and short laths. Earlier, Hill et al. [5] reported that an addition of 0.8%B or 3.08%B changed the morphology of the α-Ti phase in as-cast Ti-TiB composites.

In α-β or near β Ti alloys, the morphology of the α-Ti phase exerts an important influence on the ductility of the alloy, where equiaxed or globular α-Ti grains are in favour of acicular α-Ti grains [6, 7]. As a result, subsequent thermo-mechanical processing is often used to change the morphology of the α-Ti phase [5]. The modification effect of B offers a simple approach to the control of the morphology of the α-Ti phase in as-sintered PM Ti materials. However, no quantitative experimental analyses have been reported yet in this regard. In addition, although both the grain boundary pinning effect of TiB and the nucleation effect of α-Ti on TiB have been proposed [3, 5], no detailed theoretical or experimental support has been given yet. This paper presents a quantitative study of the effect of a small addition of B

on the modification of the morphology of the α-Ti phase and the microstructural refinement in PM CP-Ti (Grade 2), Ti-6Al-4V and Ti-10V-2Fe-3Al, which represent α, α-β and near β Ti materials, respectively. The mechanisms relevant to the microstructural changes are discussed.

2. Material and methods

The powder materials used are summarized in Table 1. The Al powder was added to balance the composition of Ti-6Al-4V due to the use of the 58V-42Al master alloy. The B powder was introduced in the range from 0.1% to 0.5%. Powder blends were prepared in a Turbula mixer for 30 min and then pressed uniaxially in a floating die into cylinder samples. Sintering was conducted at 1350 ºC for 120 min in a tube furnace under a vacuum of 10^{-3}-10^{-2} Pa, heated and cooled both at 4 ºC/min. Differential scanning calorimetry (DSC, Model Netzsch STA 409CD, Germany) was used to determine the effect of B on the phase transformation sequence in flowing high purity argon.

The microstructure of each etched sample was examined using scanning electron microscopy (SEM, Model JEOL 6460L, Japan). The average prior-β grain size was measured from 500 grains while the average length and aspect ratio of the α-Ti laths were measured from 1000 α-Ti laths using a software Image-Pro plus 5.0 statistic tool. Samples for transmission electron microscopy (TEM, Model Tecnai F20, FEI, America) characterization were cut from as-sintered specimens, ground and finally polished into 3 mm diameter small disks. They were further thinned using a precise ion polishing machine with a low-angle (<6°) and low-energy (<4 keV) ion beam. Thermo-Calc Software AB (2008) and Ti-alloys database V3 (TTTI3) were used for the thermodynamic assessment of the Ti-B system.

3. Results and discussion

Figure 1(a)-(i) shows the as-sintered microstructures of CP-Ti, Ti-6Al-4V and Ti-10V-2Fe-3Al with and without an addition of 0.3%B. Significant microstructural refinement occurred in each case. In addition, the α-Ti phase changed from long laths to a mixture of near equiaxed α-Ti grains and shorter α-Ti laths in the as-sintered Ti-6Al-4V-0.3B. Similar observations were made in the as-sintered Ti-10V-2Fe-3Al-0.7B alloy as shown in Fig. 1(j) and (k).

A detailed quantitative analysis of the as-sintered microstructures versus the addition of B is shown in Fig. 2. The prior-β Ti grain size exhibited a significant reduction at an addition of 0.1%B (see Fig. 2a), beyond which the reduction continued but at a much lesser degree. Similar observations were made of the average length and aspect ratio of the α-Ti laths in Ti-6Al-4V and Ti-10V-2Fe-3Al (see Fig. 2b).

Ti and B may form different types of borides including TiB, Ti_3B_4 and TiB_2 according to the Ti-B phase diagram, depending on the concentration of B and temperature. In the present study, small additions of B resulted in the formation of TiB, rather than TiB_2. The TEM results in Figure 3 confirmed this, where selected area electron diffraction (SAED) patterns showed a typical orthorhombic crystal structure of TiB. The in situ formed TiB particles were observed at two primary locations in each as-sintered microstructure: inside the α-Ti phase and outside the α-Ti phase. In as-sintered CP-Ti, being outside the α-Ti phase means being present along the prior-β grain boundaries while in as-sintered Ti-6Al-4V and Ti-10V-2Fe-3Al alloys being outside the α-Ti phase means being inside the β-Ti grains. The distribution of the TiB particles in different phases was quantified according to this principle. Figure 2(c) and 2(d) shows the analyses. In general, more than 60% of the TiB particles were found inside the α-Ti phase, irrespective of the addition of B and alloy composition. In particular,

more than 90% of the TiB particles were found inside the α-Ti phase in the as-sintered Ti-6Al-4V-xB alloys (x = 0.1 - 0.5), indicating a close correlation between the number of the TiB particles and the number of the α-Ti grains.

Figure 3 (a)-(c) are TEM bright field images of the TiB particles found inside some α-Ti grains in as-sintered CP-Ti-0.3B, Ti-6Al-4V-0.3B and Ti-10V-2Fe-3Al-0.3B and the corresponding SAED patterns. The interfaces between TiB and α-Ti analyzed in each alloy showed good interfacial bonding and the following preferred orientation relationships (ORs) were determined from the SAED patterns:

For CP-Ti-0.3B: $(101)_{TiB}$ // $(0001)_{\alpha\text{-}Ti}$, $[\bar{1}31]_{TiB}$ // $[0\bar{1}10]_{\alpha\text{-}Ti}$

For Ti-6Al-4V-0.3B: $(001)_{TiB}$ // $(0001)_{\alpha\text{-}Ti}$, $[0\bar{1}0]_{TiB}$ // $[0\bar{1}10]_{\alpha\text{-}Ti}$

For Ti-10V-2Fe-3Al-0.3B: $(100)_{TiB}$ // $(10\bar{1}0)_{\alpha\text{-}Ti}$, $[0\bar{1}1]_{TiB}$ // $[0\bar{1}11]_{\alpha\text{-}Ti}$

These ORs differ from those reported previously in as-cast B-containing Ti materials and PM Ti-TiB MMC materials [8-12]. The exact orientation relationship between TiB and α-Ti appears to be affected by both the chemistry and the processing conditions.

Figure 4(a) shows the DSC results of the blended elemental CP-Ti-0.3B. TiB was found to form at about 700 ºC when heated at 10ºC/min. No other exothermic events were detected while the endothermic peak at 880 ºC corresponds to the α-β transformation. Owing to the limited solubility of B in β-Ti (0.044% at 1350 °C), few TiB particles will disappear once formed in the microstructure. Those that form along the grain boundaries (Fig. 1b and c) can thus effectively restrict the growth of the prior-β grains contributing to the structural refinement observed (see Fig. 1). In the case of Ti-6Al-4V-0.3B, assuming similar cross-sections, the number density of the α-Ti grains has increased by about 6 folds estimated according to the reduction in the average length of the α-Ti laths. This suggests that there has

been a similar increase in the nucleation rate of the α-Ti phase during cooling. Accordingly, we propose a heterogeneous nucleation mechanism for the formation of the near equiaxed α-Ti grains in Ti-6Al-4V-0.3B. This is based on the observation of more than 90% of the TiB particles being found inside the α-Ti grains in Ti-6Al-4V-0.3B, the identified crystallographic ORs between TiB and α-Ti, and the peritectoid nature of the Ti-B phase diagram to be discussed below.

Figure 4(b) shows a portion of the Ti-B phase diagram up to 0.1%B. A notable feature that has been overlooked previously is that there exists a peritectoid reaction at ~882.8 °C during cooling, where β-Ti + TiB → α-Ti. This reaction almost overlaps the α-β transformation (at ~881.8 °C) and is thus difficult to detect by DSC. During solidification of various alloys, peritectic systems have proven to be excellent grain refining systems [13-15], due to the inherent crystallographic ORs between the pre-peritectic phase (the solid particle) and the solid to form. Similarly, the peritectoid reaction β-Ti + TiB → α-Ti offers a unique mechanism by which TiB nucleates the α-Ti phase if their lattice parameters match well and certain crystallographic ORs exist.

The lattice parameters of TiB (orthorhombic) are a = 6.12 Å, b = 3.06 Å, and c = 4.55 Å [16]. Its b and c parameters match the a and c parameters of the α-Ti phase (hexagonal, a = 2.95 Å, c = 4.68 Å [17, 18]), respectively. In addition, a preferred OR has been established between the TiB and the α-Ti phase in as-sintered Ti-6Al-4V-0.3B and Ti-10V-2Fe-3Al-0.3B alloy as discussed earlier. An illustration of the planar matches between $(001)_{TiB}$ and $(0001)_{\alpha\text{-}Ti}$ in Ti-6Al-4V and $(100)_{TiB}$ and $(10\bar{1}0)_{\alpha\text{-}Ti}$ in Ti-10V-2Fe-3Al is constructed in Fig. 3 (d) and (e) according to the ORs identified. The lattice mismatch between the a axis of α-Ti and the b axis of TiB is 3.6% and the lattice mismatch between their the c axes is 2.8% at room

temperature. In addition, the diagonal segment "*L*" (5.9 Å) of the basal plane of the α-Ti phase matches the *a* axis (6.12 Å) of the TiB cubic very well with a lattice mismatch of 3.6%.

The preferred ORs identified in conjunction with the excellent lattice matches support the argument that crystallographically, TiB is a potent heterogeneous nucleant for α-Ti. The peritectoid reaction offers an ideal mechanism by which the α-Ti phase nucleates on the TiB particles. In principle, those TiB particles that form during heating above 700 ºC or that precipitate out from the β-Ti phase during subsequent cooling can both nucleate α-Ti. This also explains the observation that most of the TiB particles are found inside the α-Ti grains.

4. Conclusions

In summary, a small addition of boron changes the morphology of the α-Ti laths in as-sintered Ti-6Al-4V and Ti-10V-2Fe-3Al to near equiaxed α-Ti grains in addition to restricting prior-β grain growth. TiB forms at about 700 °C during heating to the isothermal sintering temperature and exists predominantly inside the α-Ti gains and at the prior-β grain boundaries in the as-sintered microstructure. The refinement of prior-β grains is due to TiB particles pinning prior-β grain boundaries. TEM characterization identified specific orientation relationships between the TiB particles and the α-Ti phase in as-sintered CP-Ti, Ti-6Al-4V and Ti-10V-2Fe-3Al. Excellent lattice matches exist between TiB and α-Ti along all major directions (mismatch <3.6%). The peritectoid reaction between the β-Ti phase and TiB, i.e. β-Ti + TiB → α-Ti, offers an ideal mechanism by which α-Ti nucleates on TiB particles and may have contributed to the enhanced heterogeneous nucleation of α-Ti on TiB. The substantially increased number density of the α-Ti grains and its near equiaxed morphology is attributed to the heterogeneous nucleation effect of the α-Ti phase on the TiB particles.

Acknowledgements - This work was funded by the Australian Research Council (ARC) through an Australian Postdoctoral Fellowship for Dr. Y. F. Yang and the Centre of Excellence for Design in Light Metals.

References

[1] M. Marty, H. Octor, A. Walder, US Patent, 4,601,874 (filed 8 July 1985, granted 22 July 1986).

[2] T. Saito, Adv. Perform. Mater. 2 (1995) 121-144.

[3] O.M. Ferri, T. Ebel, R. Bormann, Adv. Eng. Mater. 13 (2011) 436-447.

[4] S.D. Luo, Y.F. Yang, G.B. Schaffer, M. Qian, J. Alloy. Compd. 555 (2013) 339-346.

[5] D. Hill, R. Banerjee, D. Huber, J. Tiley, H.L. Fraser, Scripta. Mater. 52 (2005) 387-392.

[6] R.R. Boyer, G.W. Kuhlman, Metall. Trans. A 18 (1987) 2095-2103.

[7] G. Terlinde, H.J. Rathjen, K.H. Schwalbe, Metall. Trans. A 19 (1988) 1037-1049.

[8] M.E. Hyman, C. McCullough, J.J. Vallencia, C.G. Levi, R. Mehrabian, Metall. Trans. A 20 (1989) 1847-1859.

[9] V.K. Chandravanshi, R. Sarkar, P. Ghosal, S.V. Kamat, T.K. Nandy, Metall. Mater. Trans. A 41 (2010) 936-946.

[10] P. Nandwana, S. Nag, D. Hill, J. Tiley, H.L. Fraser, R. Banerjee, Scripta. Mater. 66 (2012) 598-601.

[11] D.X. Li, D.H. Ping, Y.X. Lu, H.Q. Ye, Mater. Lett. 16 (1993) 322-326.

[12] H.B. Feng, Y. Zhou, D.C. Jia, Q.C. Meng, J.C. Rao, Cryst. Growth Des. 6 (2006) 1626-1630.

[13] I. Maxwell, A. Hellawell Acta Metall. 23 (1975) 229-237.

[14] M. Qian, Acta Mater. 55 (2007) 943-953.

[15] B.F. Decker, J.S. Kasper, Acta Cryst. 77 (1954) 77-80.

[16] R.M. Wood, Proc. Phys. Soc. 80 (1962) 783-792.

[17] M.J. Bermingham, S.D. McDonald, K. Nogita, D.H. StJohn, M.S. Dargusch, Scripta Mater. 59 (2008) 538-541.

[18] S. Tamirisakandala, R.B. Bhat, D.B. Miracle, S. Boddapati, R. Bordia, R. Vanover, V.K. Vasudevan, Scripta Mater. 53 (2005) 217-222.

Table 1 Powder materials used

Powder materials	Particle size (μm)	Purity (%)	Manufacturer or supplier
Hydride-dehydride (HDH) Ti	≤63	99.4%	Kimet, China
66.7V-13.3Fe-20Al master alloy	≤45	99.5%	Baoji Jia Cheng Rare Metal Materials Co. Ltd., China
58V-42Al master alloty	≤45	99.5%	Baoji Jia Cheng Rare Metal Materials Co. Ltd., China
Elemental Al	~3	99.7%	Aluminium Powder Company Ltd., England
Elemental B	~1	~95%	Strem Chemicals

FIGURES AND FIGURE CAPTIONS

Figure 1 As-sintered microstructures of CP-Ti, Ti-6Al-4V and Ti-10V-2Fe-3Al with and without an addition of B, sintered at 1350 ºC for 120 min in vacuum: (a) CP-Ti; (b) CP-Ti-0.3B; (c) an enlarged view of (b); (d) Ti-6Al-4V; (e) Ti-6Al-4V-0.3B; (f) an enlarged view of (e); (g) Ti-10V-2Fe-3Al; (h) Ti-10V-2Fe-3Al-0.3B; (i) an enlarged view of (h); (j) Ti-10V-2Fe-3Al-0.7B; (k) an enlarged view of (j).

Figure 2 (a) Average prior-β grain size in as-sintered CP-Ti-xB, Ti-6Al-4V-xB and Ti-10V-2Fe-3Al-xB (x = 0, 0.1, 0.3, 0.5), (b) average aspect ratio of the α-laths in as-sintered Ti-6Al-4V-xB and Ti-10V-2Fe-3Al-xB (x = 0, 0.1, 0.3, 0.5); (c) distribution of the TiB particles inside the α phase, and (d) distribution of the TiB particles along grain boundary. Ti64 stands for Ti-6Al-4V while Ti1023 refers to Ti-10V-2Fe-3Al.

Figure 3 TEM bright field images and SAED patterns of the TiB particles observed inside some α-Ti grains in the as-sintered microstructures of: (a) CP-Ti-0.3B, (b) Ti-6Al-4V-0.3B and (c) Ti-10V-2Fe-3Al-0.3B. (d) and (e) are illustrations of the planar matches with the identified orientation relationships: (d) $(001)_{TiB}$ // $(0001)_{\alpha\text{-}Ti}$, $[0\bar{1}0]_{TiB}$ // $[0\bar{1}10]_{\alpha\text{-}Ti}$ existing in Ti-6Al-4V-0.3B and (e) $(100)_{TiB}$ // $(10\bar{1}0)_{\alpha\text{-}Ti}$, $[0\bar{1}1]_{TiB}$ // $[0\bar{1}11]_{\alpha\text{-}Ti}$ existing in Ti-10V-2Fe-3Al-0.3B.

Figure 4 (a) DSC curve of CP-Ti-0.3B, heated to 1400 ºC at 10 ºC/min in flowing argon and (b) Ti-B phase diagram up to 0.1% B produced using Thermo-Calc Software AB (2008) and Ti-alloys database V3 (TTTI3).

Figure 1

Click here to download high resolution image

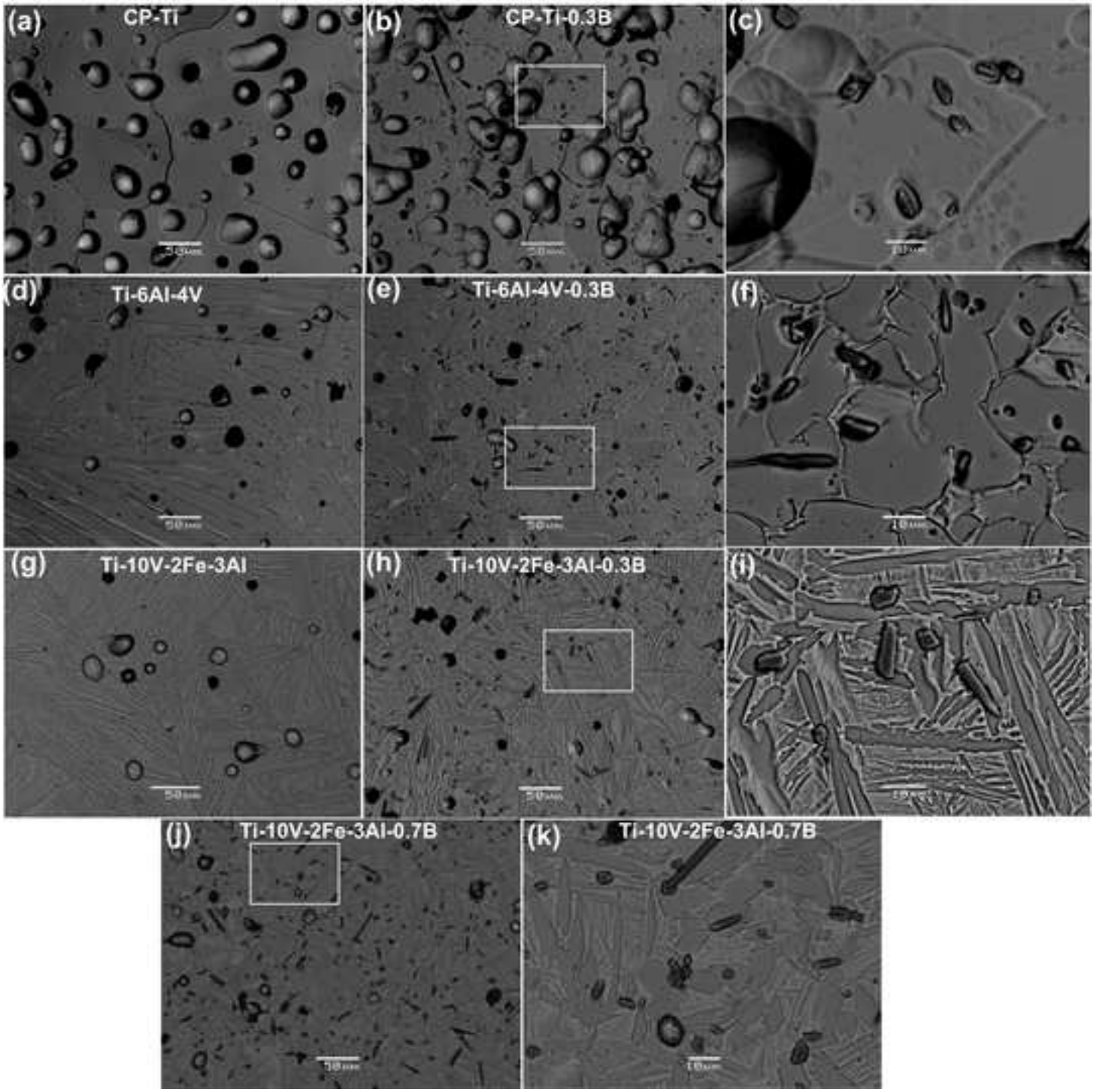

Figure 2

Click here to download high resolution image

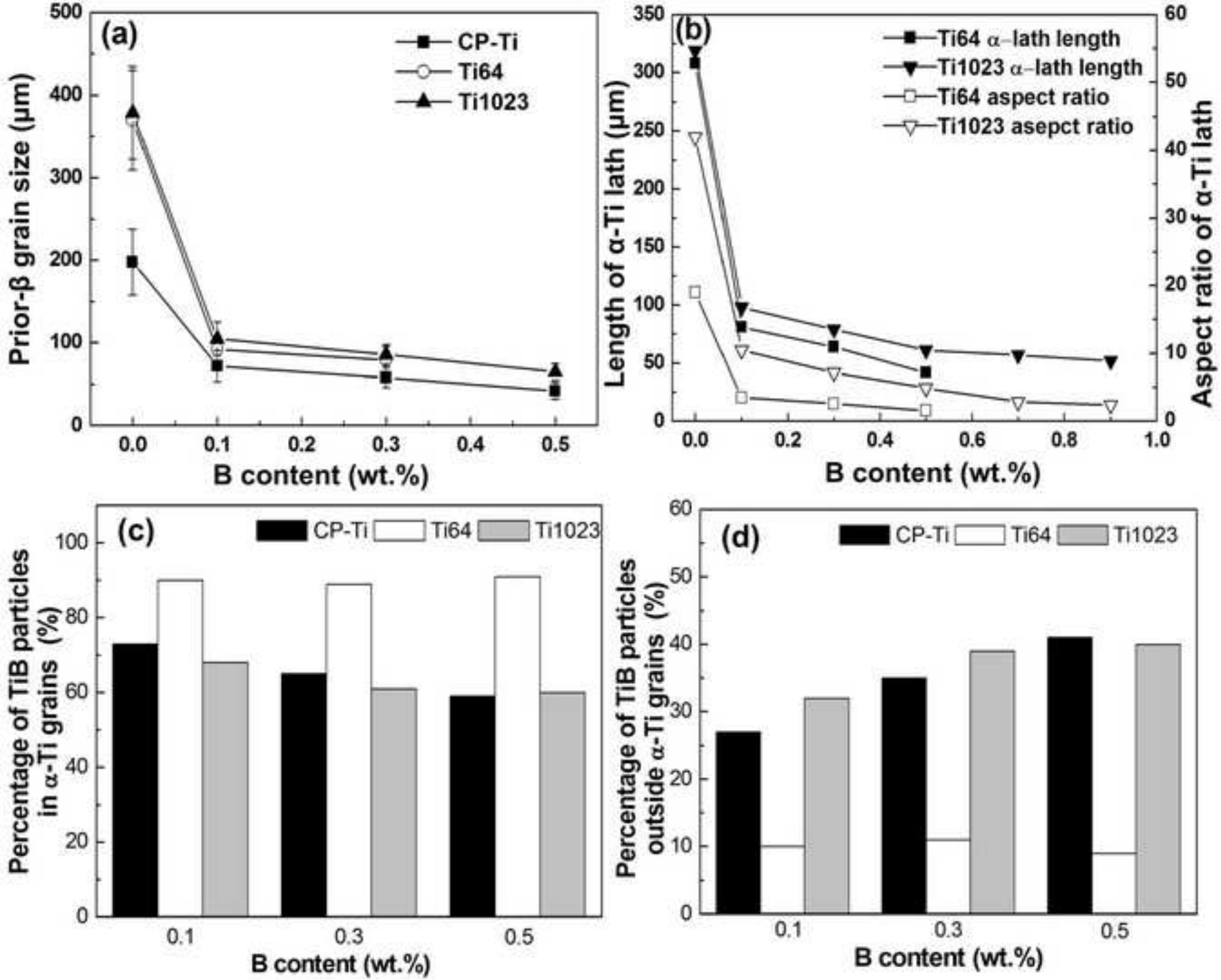

Figure 3

Click here to download high resolution image

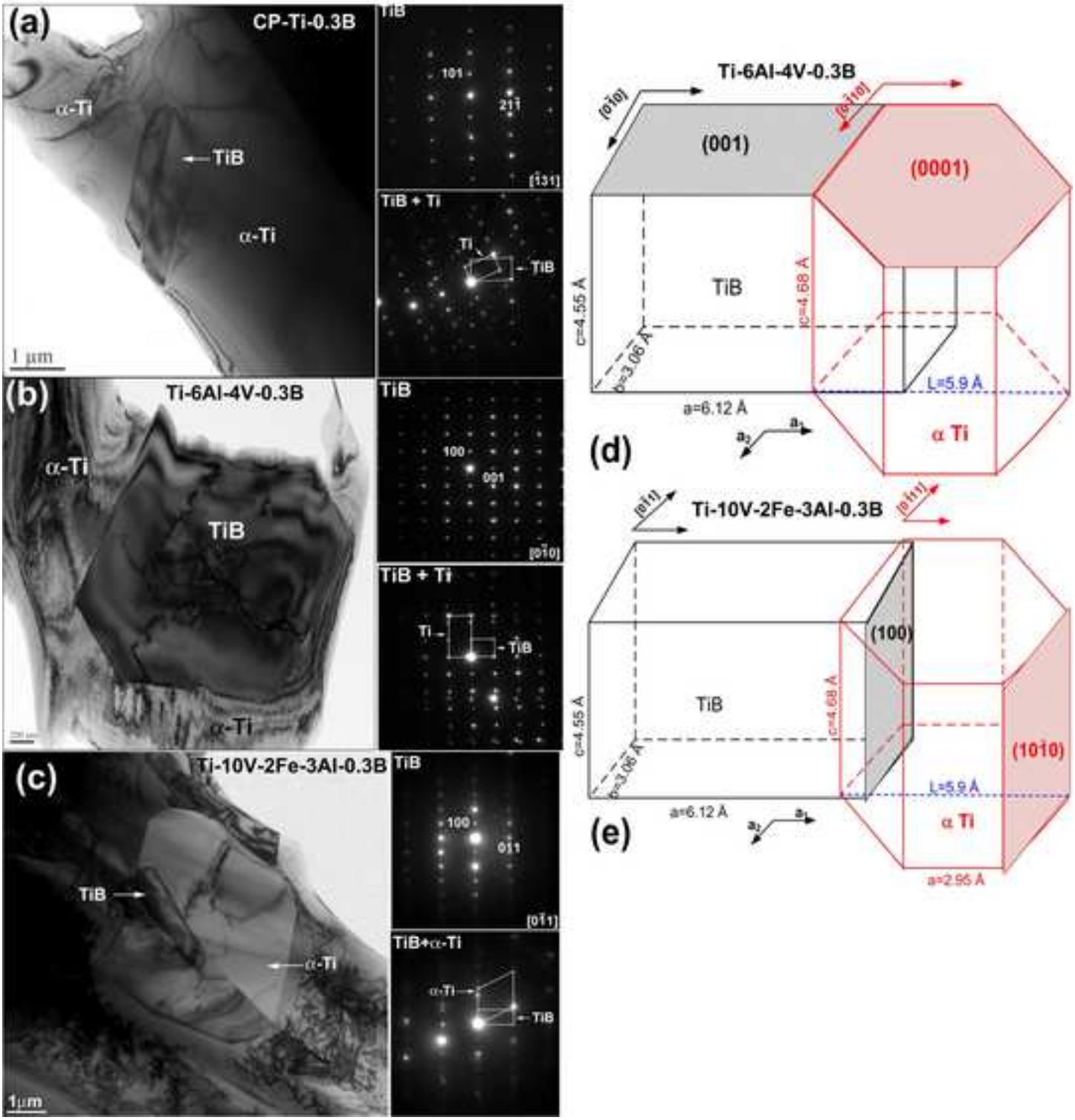

Figure 4

Click here to download high resolution image

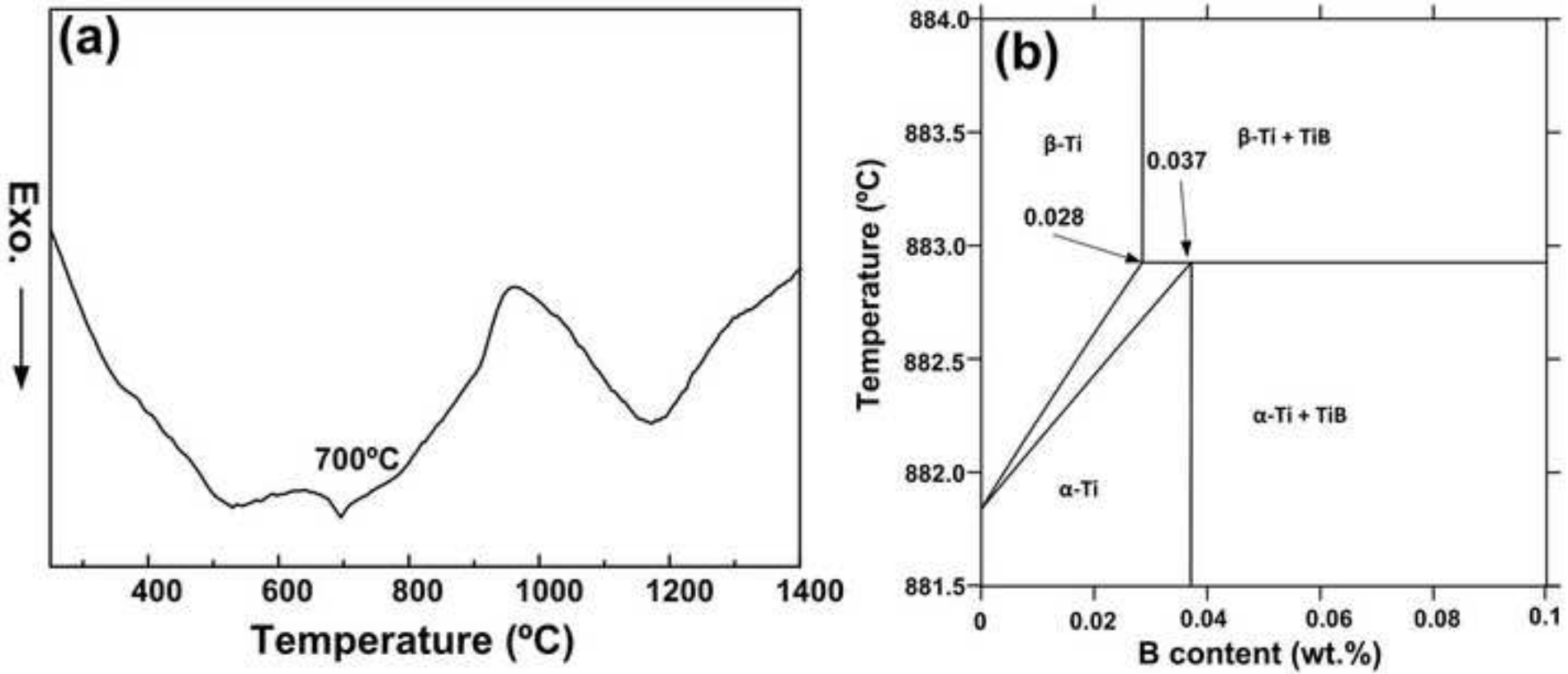

highlight

Click here to download Supplementary Material: highlights.docx